Refining sperm quality assessment by high-throughput nuclear morphometric analysis

Abstract

Artificial insemination (AI) is commonplace in commercial pig breeding, and as such, ensuring sperm sample quality is of utmost importance to avoid reduced farrowing rates and litter sizes. Here, we have used high-throughput nuclear morphometric analysis to compare pig sperm samples categorised as meeting the AI standard (AIS) or not meeting the AI standard (N-AIS). We find that pig sperm nuclei are asymmetric, and that samples contain phenotypic shape abnormalities that show continuous variation. Samples classed as N-AIS have more abnormally shaped sperm than AIS samples, but conventional analysis misses many. The specific phenotypes identified suggest aspects of spermiogenesis that may be disrupted and indicate future avenues for improving pig sperm quality. This method reveals a significant difference in sperm head morphology between AIS and N-AIS pig sperm samples and has the potential to be further developed as a high-throughput tool for sperm head morphology assessment both in the pig breeding industry and in other species.

Keywords: Artificial insemination, morphology, nucleus, pig, sperm

Background

Infertility, defined as the failure to achieve a pregnancy after one year of regular unprotected sexual intercourse, will affect around one in six people. Between 20 and 30% of these cases result solely from male factor infertility, with up to 50% of all instances being at least partly the result of male factor infertility [1]. The analysis of semen parameters is an important part of infertility investigations, with semen volume and pH being documented, and sperm parameters such as concentration, progressive motility and morphology all being routinely observed [2]. Many of these factors are determined during spermatogenesis, the complex process by which undifferentiated diploid spermatogonia become highly specialised haploid spermatozoa, with the process involving complicated cellular, proliferative, and developmental phases [3]. Which single sperm parameter is the most important for fertility is a source of conflict in the literature. Some studies, for example, suggest that sperm progressive motility is positively associated with pregnancy rates [4,5], whilst others do not [6]. Similarly, research has indicated that sperm morphology may be correlated with positive pregnancy outcomes [7–9], but others have suggested that this plays less of a role than previously thought [10].

In agriculturally important species such as pigs, cattle, and sheep, semen analysis followed by artificial insemination (AI) is commonplace in breeding programmes [11], with 90% of sows in the world's primary pork producing countries resulting from AI [12]. As such, an industry-led working code of practice, the AI standard for pigs has been developed to assure standards of AI are received by pork producers in the UK [13]. Generally, the goals of agricultural animal breeding are to maximise the production of meat at a low cost, and to

43 efficiently disseminate the genetics of particularly valuable animals. As such, the use of high-
44 quality semen doses is of paramount importance, for example in pigs the use of lower-
45 quality doses is associated with lower farrowing rates and smaller litter sizes [14,15]. The
46 fast identification of animals that consistently produce N-AIS samples is therefore important
47 to ensure their removal from breeding programmes; it has been shown for example that
48 boars with fertility problems in a nucleus herd have the potential to reduce litter sizes
49 throughout the entire breeding population [16], in part due to one boar ejaculate commonly
50 being used to serve between 15 and 25 sows [17] in routine AI. Semen parameters are
51 therefore of key importance both in human fertility assessment and treatment and in
52 agricultural practice.
53
54 As is the case for all mammals, an ejaculate from a boar, bull or ram does not contain a
55 homogenous population of sperm [18] making analysis and the subsequent identification of
56 subfertile individuals, challenging. In the general analysis of boar sperm morphology for
57 example, a sample is deemed to be “fertile” if the frequency of abnormal sperm heads does
58 not exceed 10%. Fertility can also be assumed if the frequency of abnormalities in
59 acrosomes, mid-pieces, tails, or proximal cytoplasmic droplets is less than either 5% each, or
60 15% when combined [19]. In humans, the percentage of normal forms (in both fertile and
61 subfertile men) is usually far less than 30% [20], and has been documented to be
62 consistently (and staggeringly) low, with only 3-5% normal forms being identified in assisted
63 reproductive technology (ART) cases [9,21,22].
64

65 There also remains much to learn about mammalian sperm biology. Only a limited number
66 of studies to date have focused on the analysis of sperm nuclear morphometry in
67 agricultural animals [23,23,24], and whilst it has previously been shown that sperm shape
68 differs between high and low fertility bulls [25], such observations are limited in pigs [26,27]
69 and differences in morphometric variables that may be related to pig fertility are yet to be
70 elucidated [28]. Whilst the goals of the livestock industry are in stark contrast to human
71 fertility treatment, furthering our understanding of the biology of sperm in general has
72 potential benefits for both fields. Here, we have used Nuclear Morphology Analysis (NMA)
73 [29–33], morphometrics software for microscopy images, to measure and compare the
74 shapes of sperm nuclei from 21,002 pig sperm cells. This is the largest reported number of
75 individual sperm nuclei that have been analysed at this level of detail in any agricultural
76 animal. Our objective is to understand how sperm shape relates to samples being classified
77 as AIS or N-AIS, and to determine if certain sperm features can be correlated with specific
78 biological processes. If these differences can subsequently be linked to fertility, such
79 analysis has the potential to provide an alternative to the livestock industry standard
80 practices and may provide transferrable insights into human sperm morphology.
81

82 **Methods**

83 *Semen collection*

84 Fresh ejaculated sperm samples from boars were collected using the gloved hand method
85 [34], by trained staff at JSR Genetics Ltd. Samples were stored in Duragen extender,
86 supplemented with no less than: 500 IU per ml streptomycin; 500 IU per ml penicillin; 150
87 mg per ml lincomycin; and 300 mg per ml spectinomycin, diluted to 2.3 billion sperm per

88 dose. Samples were stored at 17°C and were prepared within two days of collection. No
89 specific ethical approval was required for this study as all semen doses used were collected
90 as part of JSR Genetics Ltd.'s standard commercial procedures. Semen samples identified as
91 N-AIS by the industry were discarded, and those that were identified as AIS by the industry
92 were used commercially.
93
94 *Sample preparation*
95 Prior to preparation of samples for this study, semen samples were identified as either AIS
96 or N-AIS using computer assisted sperm analysis (CASA) followed by manual assessment at
97 JSR Genetics Ltd. Specifically, samples that had a morphology score of above 70% (obtained
98 from CASA) and a motility score of above 4 (1 to 5, 1 being dead and 5 being excellent
99 progressive forward movement) were graded as AIS and those falling below these criteria
100 were graded as N-AIS.
101
102 50 AIS and 44 N-AIS samples were used in this study. 2ml of each semen sample was
103 centrifuged at 300g for 5 minutes at 17°C. The supernatant was discarded, the pellet was
104 resuspended in 1.5ml of fixative solution (100% methanol and 100% acetic acid, added
105 dropwise at a 3:1 ratio) and centrifuged at 300g for 5 minutes at 17°C. The supernatant was
106 discarded, and the pellet was resuspended in 1.5ml of fixative solution. 10µl of each sample
107 was then dropped onto the centre of the surface of a labelled (sample ID, date), steam-
108 warmed slide, immediately followed by 10µl of fixative solution. Subsequently, slides were
109 air-dried for two minutes before one drop of fluorescent DAPI (4',6-diamidino-2-

110 phenylindole) was added to the centre of the slide. Prepared slides were air-dried in the
111 dark, for at least 20 minutes prior to microscopy.
112
113 *Image acquisition*
114 An Olympus IX83 inverted fluorescence microscope equipped with a XM10 monochrome
115 CCD camera and CellSens Dimension version 1.9 (expandable imaging software for Life
116 Science microscopy) was used for image capturing. A minimum of 200 nuclei per sample
117 were imaged at 1000x magnification.
118
119 *Data analysis*
120 Images were analysed using Nuclear Morphology Analysis (NMA) v2.2.1 [30,33], available
121 here). This software enables automated recognition of round or asymmetric nuclei within an
122 image of interest, and the subsequent morphological analysis of these nuclei. We adapted
123 the landmark recognition to detect and analyse pig sperm nuclei. The software generates
124 'profiles' describing the interior angles around the perimeter of the nucleus, and the
125 diameter and radii across the centre of mass (Figure 1). Pig sperm are (mostly) symmetrical
126 about the anterior-posterior axis, and the tail attachment region, characterised by a 'dimple'
127 in the nucleus, was chosen to anchor the profiles and orient the nuclei (Figure 1A, reference
128 point 1).

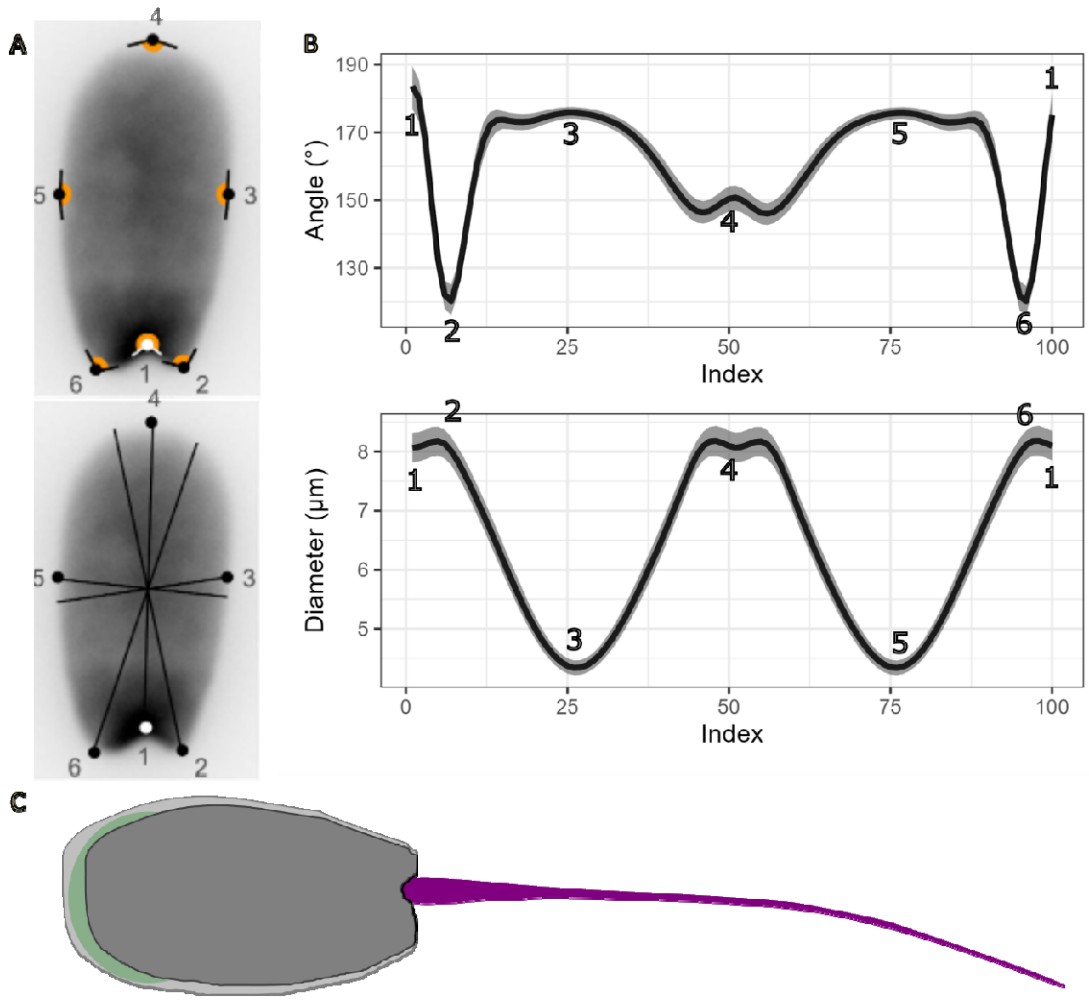

Figure 1 – Example morphometric profiles of pig spermatozoa. A) angle profiles measure the internal angle around the perimeter of the nucleus. Diameter profiles measure diameter across the centre of mass. The numbered points are indicated in the profiles, demonstrating key landmarks can be identified. B) Profiles show median and interquartile range of the angles and diameters of cells. C) schematic of a pig spermatozoon; the sperm nucleus (dark grey) fills most of the sperm head, with the remainder of the head comprising the acrosome (green) and the residual cytoplasm (lighter grey). The tail (purple) is not

shown to scale but is included to illustrate the attachment region.

For consistent alignment of the nuclei, the tail attachment region (as can be seen in Figure 1 A point 1 and 1C) was placed directly below the centre of mass of the nucleus.

Data was exported from NMA and further processed in R (4.4.0) [35] using a custom analysis pipeline. Initially, k-means clustering on diameter profiles was used to identify distinct groups of shapes, with dimensionality reduction using UMAP [36,37] employed to visualise the shape profiles. Continuous phenotypes were then detected by selective focus on outlier cells, detected using the angle, radius and diameter profiles (Figure 1B).

Cells were classed as normal or abnormal using the profile data. Each profile contains 100 indexes (Figure 1A and 1B); at each index, potentially abnormal cells were detected as those cells with values outside 1.5x the interquartile range. Cells were then scored on how many indexes met the criteria for abnormality. Consistent abnormal phenotypes have higher values, while more normal phenotypes have lower values. For each profile, the cells with a score higher than the mean number of abnormal indexes were determined to be morphological outliers. This allowed us to identify continuous morphological variation across cell populations. Cells were assigned a grouping of ‘normal’ (not identified as outliers), ‘intermediate abnormality’ (the cell was an outlier across a single profile type) or ‘extreme abnormality’ (the was an outlier across multiple profile types).

150 Associations of breed, sample and date of collection with the severity of phenotype were
151 tested using a Scheirer-Ray-Hare test (a non-parametric equivalent to a two-factor ANOVA).
152 A significant association prompted the use of ordinal logistic regression to explore the
153 association further. The samples were filtered to only known breeds and collection dates for
154 which all samples had data (9321 cells). Ordinal logistic regression was implemented with
155 the *polr* function in MASS [38] using a negative log-log link to account for higher proportions
156 of normal phenotypes, modelling the phenotype cluster as the interaction of collection date
157 and sample. The proportional odds assumption of the model was tested with the Brant-
158 Wald test, and an intercept-only model was created to test the null hypothesis that the
159 predictor variables added no information.
160
161 The predictive ability of morphometric data to classify samples as either AIS or N-AIS was
162 tested using logistic regression via generalised linear models. Two models were created; the
163 first using standard industry measurements (width, perimeter, area, ellipticity, elongation,
164 roughness, regularity and height [19,39]), and the second using the morphometric profiles
165 (angle, radius and diameter), modelling a sperm class as dependent on the morphometric
166 parameters. The samples were split into training (70%) and test (30%) groups. The
167 probability of being in the AIS group was calculated for each sperm in a sample, and the
168 mean probability was taken as the overall sample value.
169
170 Figures were generated using ggplot2 [40],UMAPs were generated using the UMAP package
171 [36,37], Factoextra was used for heirarchicdal clustering and Caret was used for GLM
172 validation. Scripts used in this analysis are available here.

173

174 **Results**

175 *Pig sperm samples contain continuous phenotypic abnormalities*

176 Analysis of sperm nuclear morphology from 50 AIS ejaculates and 44 N-AIS ejaculates

177 yielded measures from 11,416 and 9,586 nuclei, respectively. Comparisons between these

178 groups of animals indicated that sperm heads differ, but that there is a large amount of

179 overlap and variation between individuals (Figures S1-4).

180

181 To identify different nuclear shape phenotypes in the samples, all samples were combined

182 into a single dataset to enable a full unbiased comparison of shapes. The first global

183 observation indicated that sperm fell clearly into two equal sizes groups with distinct shape

184 profiles (Figure 2A).

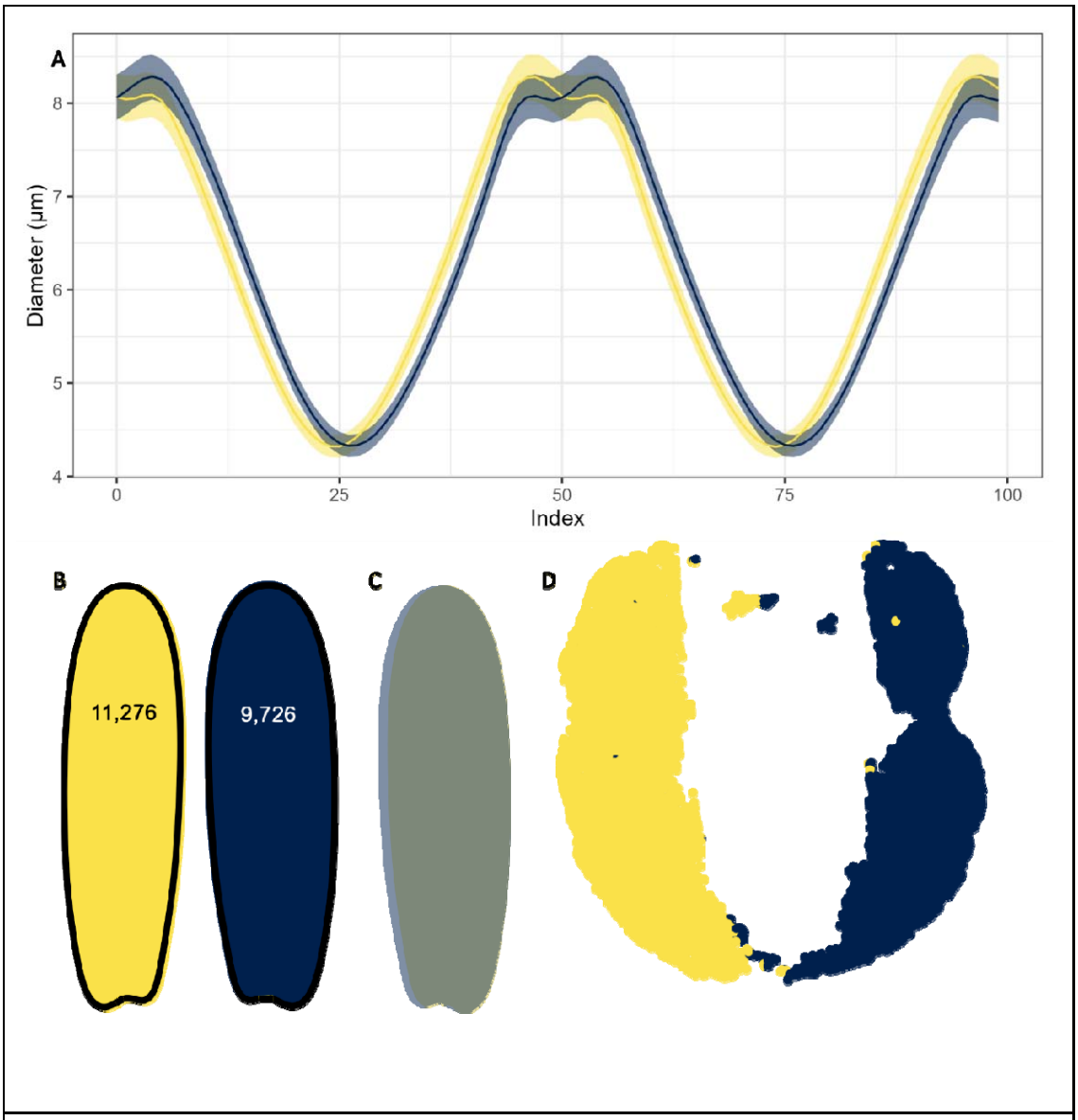

Figure 2. Cell shapes fall into two equally sized groups with mirroring around the vertical axis; A) diameter profiles for each cluster show the symmetrical clusters B) Consensus nucleus shapes show the main difference is at the tail attachment region with the more prominent side to the left or right respectively. C) the left cell in B mirrored across the vertical axis and overlaid on the right cell shows the two cell populations are mirrors of each other. D) Dimensionality reduction of diameter profiles by UMAP shows almost all

cells fall cleanly into these two groups.

185

186 These two groups of sperm cells correspond to the differences in the shape of the tail
187 attachment region, which is compressed on either the left or the right side (Figure 2B). The
188 profiles of the nuclei with compression on the right side were reversed to determine if the
189 shapes were mirrored and superimposable. The two groups are indeed mirror images of
190 each other around the tail attachment region (Figure 2C), and almost all cells in the dataset
191 fall neatly into these two major groups (Figure 2D). This, plus the general inflexibility of
192 sperm chromatin, suggests the differences are unlikely to be due to compression from the
193 angle of the tail at the time of fixation. Rather, the nucleus appears truly asymmetric, and
194 the difference we observe is caused by the sperm head falling on its dorsal or ventral
195 surface when the slide was prepared.

196

197 Since the shape around the tail attachment region was the primary factor that separated
198 nuclei of different shapes, and UMAP showed continuous variation, standard clustering *e.g.*
199 [41] to identify discrete shape groups was not feasible. Instead, we aggregated outlier nuclei
200 with similar shape profiles to identify continuous phenotypes, iteratively grouping nuclei
201 with the greatest differences to normal profiles. This amalgamation of outlier shapes
202 yielded a normal phenotype group (containing 85.2% of nuclei), an intermediate phenotype
203 group (12.7%) and an extreme phenotype group (2.1%). The progression from intermediate
204 to extreme involved condensation of the basal region and bulbing of the anterior region
205 (Figure 3) with two main pathways; one being the compression with failure to elongate

206 resulting a short pyriform phenotype (Figure 3A;7.75%) and the other being abaxial tail
207 attachment and basal compression resulting in an abaxial pyriform phenotype (Figure
208 3C;6.25%). The intermediate phenotypes are the hardest to categorise as the vary from with
209 minor tapering at the basal region that is difficult to detect to the relatively well-formed side
210 of the spectrum of pyriform cells. This spectrum makes up the largest portion of the
211 abnormality in pig sperm and is highly variable, containing cells that are either the
212 intermediates of a spectrum of abnormality or the end of more minor morphological
213 changes. There is also within the intermediate phenotypes minor tapering and formation of
214 spikes in the basal region (Figure 1B; 1%).

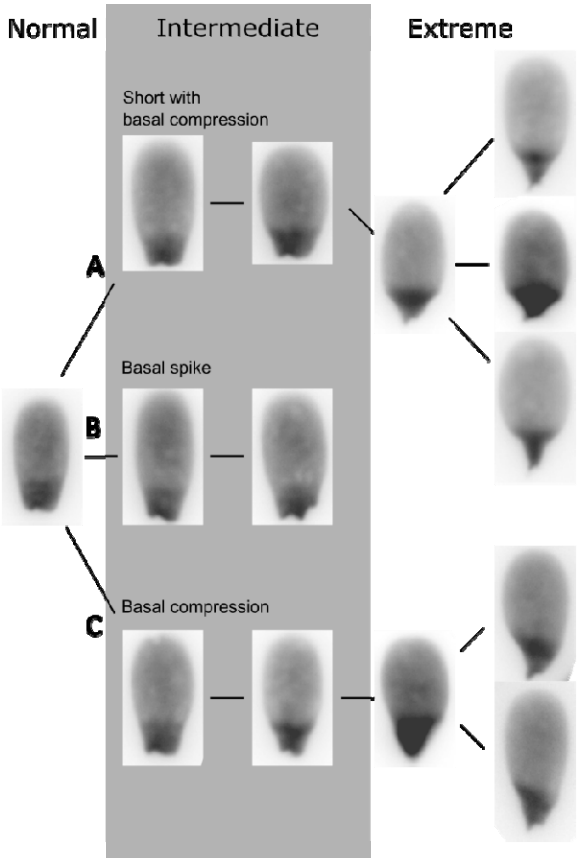

215

216 Figure 3. Example DAPI stained images of progressively abnormal sperm phenotypes. Three
217 main classes of abnormality can be seen: A) short (compression anterior-posterior, leading
218 to reduced bounding height) progressing to compression (tapering) around the base of the
219 nucleus and a pyriform phenotype; B) extrusion of nuclear DNA forming a spike near the
220 base of the nucleus with some tapering; C) abaxial compression (tapering) around the base
221 of the nucleus, leading to a pyriform phenotype.
222
223 *AIS and N-AIS samples both contain abnormal sperm phenotypes*
224 Our initial analysis indicated that *c.*15% of the sperm were abnormally shaped, but, as
225 samples were pooled, this did not indicate if these were enriched in the N-AIS samples or if
226 their abundance related to other characteristics of the samples. images showing the
227 progressive phenotypes from normal to extreme are shown in Figure 1. We therefore
228 looked at three characteristics: the sample's status as AIS or N-AIS, the breed of the boar
229 (where known, n= 11,448 sperm heads) and the date of sample collection (as a proxy for
230 environmental or technical factors). Intermediate and extreme sperm phenotypes were not
231 evenly distributed across all samples (Figure 4), and while the abnormal phenotypes were
232 more prevalent (1.96:1 N-AIS:AIS more extreme, 1.44:1 N-AIS:AIS more intermediate) in the
233 N-AIS samples, they were also found in AIS samples.
234

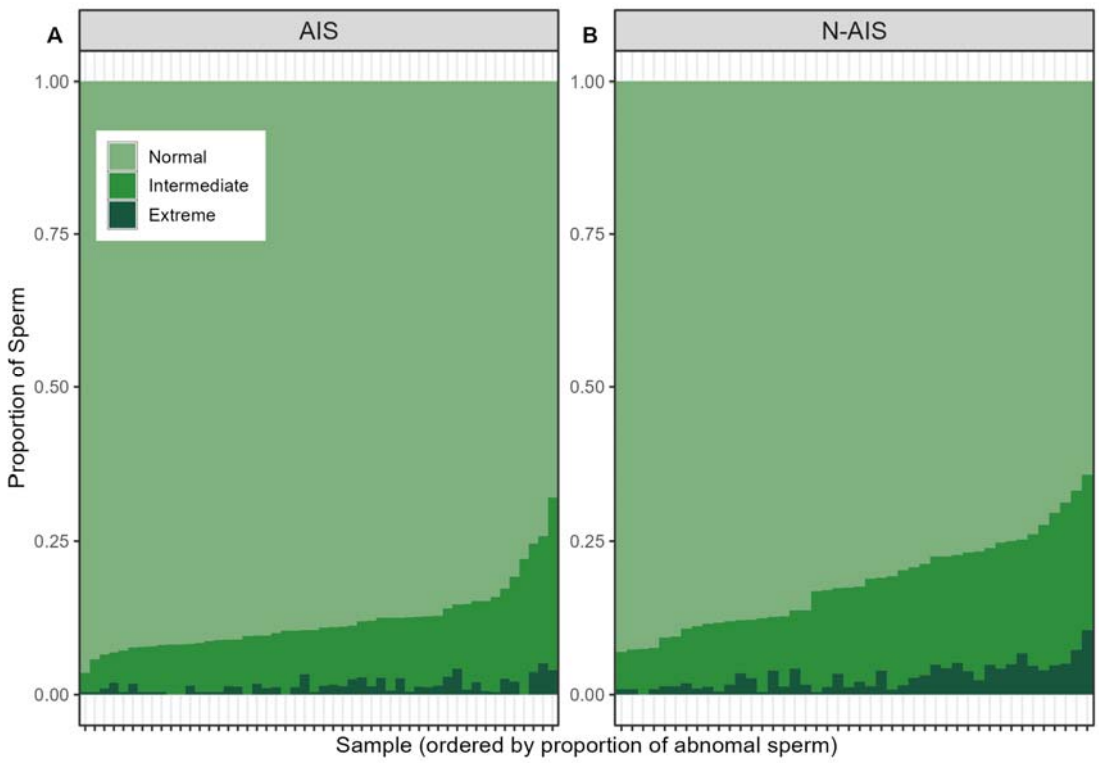

Figure 4 – Proportion of sperm in normal, intermediate or extreme groups for A) AIS samples (50 samples) and B) N-AIS samples (44 samples). Intermediate and extreme phenotypes are more frequent in N-AIS samples but are also common in a subset of the AIS samples.

235

236 Given that the pattern of data suggested there was variation between samples and between
237 sample collection dates (Figures S3 and S4), we tested whether the distribution of
238 phenotypes could be associated with the date of sample collection or individual samples
239 across the entire dataset. Significant associations were found for both variables and their
240 interaction (Scheirer-Ray-Hare test, $p<0.001$ for each). To explore the interactions in more
241 detail, we focussed on the samples for which breed was known. We then selected dates for

242 which all these breeds were present. Ordinal logistic regression did not reveal a global
243 association between the severity of the phenotype and the individual sample for the known
244 breeds ($p>0.05$) apart from White Duroc ($p=0.01$) in which severe phenotypes were more
245 common (Table S1). The odds that a sperm cell had an extreme phenotype versus
246 intermediate or normal was increased 2.1 times compared to other breeds.
247
248 The date of collection had some global associations with severity of phenotype; for
249 example, for samples collected on one date (6th July), the odds that a sperm cell had an
250 extreme phenotype versus intermediate or normal was increased 3.3 times compared to
251 other dates ($p<0.001$). Most other dates did not show global effects.
252
253 Interaction effects were detected between the date of collection and individual samples
254 (see Table S1 for a full breakdown), indicating that the environment has a larger impact on
255 the quality of the ejaculate than the breed of the boar. This was confirmed by testing for
256 differences in the shape profiles between breeds. Repeated Wilcoxon rank-sum tests,
257 multiple testing corrected with the Holm method showed no significant difference in the
258 angle, radius or diameter profiles between breeds suggested that there is subtle nuclear
259 morphological variation between breeds, with differences dominated by shared genetic or
260 environmental factors.
261
262 *Classification of normal/abnormal cell types does not align with industry assigned AIS/N-AIS*
263 *classifications*
264

265 We next considered if the extra morphometric information measured allowed for more
266 robust classification of samples as AIS/N-AIS than is currently possible. The samples were
267 originally classified based on motility and shape, with 70% morphologically normal forms
268 and a motility score of above 4 leading to a classification of AIS. Although motility
269 information was not available for these samples, the predictive power of conventional
270 morphometrics was compared. For this, a GLM was created to predict the probability of a
271 cell as originating from an AIS or N-AIS sample based on the width, perimeter, area,
272 ellipticity, elongation, roughness, regularity and height, as are commonly used in industry.
273 Each sample was scored as the mean of its individual cell predictions (Figure S2A). This score
274 was then compared to a GLM that used the shape profiles for prediction (Figure S2B). This
275 comparison indicated that greater discrimination between the AIS and N-AIS samples was
276 possible. The ability to classify samples directly by the proportion of normal, intermediate or
277 extreme phenotypes is in principle a useful improvement on the simpler morphometric
278 measures; AIS samples with a high rate of shape abnormalities in particular show that there
279 is morphological variation present that needs to be further explored.
280

281 **Discussion**

282 *Continuous sperm shape phenotypes unify previous understanding of pig sperm variation*
283 Studies of pig sperm shape, and indeed the sperm of other species, usually focus on simple
284 morphometric measurements such as area and circularity [19,28,42–44]. However, these
285 measures can miss subtle phenotypes, especially when large numbers of sperm are being
286 screened. Here, 21,002 sperm nuclei have been analysed at high resolution allowing in-
287 depth comparison of sperm nucleus shape. Previous pig sperm morphology studies report

288 the analysis of between 3,000 and 5,550 sperm heads [43,45]. To the best of our
289 knowledge, this is therefore the largest reported number of individual sperm nuclei that
290 have been analysed at this level of detail in any agricultural animal. The use of this large
291 sample size has allowed us to detect and characterise subtle phenotypes that have
292 previously been overlooked.
293
294 Previous studies measuring bright-field images have identified differences in sperm head
295 size between pig breeds with Saravia *et al.* concluding that Duroc sperm heads were 0.2µM
296 longer and 0.1µM wider than other tested breeds [19], and Kawarasaki, Enya and Otake
297 finding Duroc sperm heads to be 0.1µM longer and 0.03µM wider [45]. Given that such
298 differences were not observed here (Figure S1), the size difference seen in other studies
299 may be due to the structures outside of the nucleus, or due to sample variation. Of note
300 however, is that the Duroc pig samples analysed in this study were from crossbred white
301 Duroc animals. This crossbreeding may have resulted in the smaller sperm observed due to
302 a lack of genetic diversity or a potential founder effect (Figure S1).
303
304 As shown in Figure 2, asymmetry in pig sperm nuclei was identified, with one side of the tail
305 attachment being consistently larger than the other. Given that pig sperm nuclei are
306 flattened, we conject that this asymmetry reflects how the sperm cells fell on the slide
307 during preparation; either dorsally or ventrally. Evidence from scanning electron microscopy
308 also suggests that the asymmetry is present in the full sperm head, not just the nucleus [45].
309

310 The other shape phenotypes that were discovered in this study were continuous, with
311 progressive abnormalities involving compression around the base of the nucleus (Figure 3).
312 Some of these shape phenotypes are similar to those reported before, including the division
313 of intermediate and extreme phenotypes [43,45,46].
314
315 Basal nucleus compression causing a bulb-like shape has been observed in the sperm of
316 other species such as humans [46], and has been studied extensively in cattle [47–51].
317 Notably, *Kif3a* knockouts in mice have also been shown to generate similar sperm
318 phenotypes [52], although much of the characterisation of sperm phenotypes to date has
319 been either manual or using CASA systems measuring simple morphometric values, and
320 therefore lack the power required to detect subtle variations [23,24,28,43,45,53,54].
321
322 Some of the samples with the greatest proportion of abnormal sperm were collected on the
323 same day, suggesting that environmental factors, either pre- or post- sample collection, may
324 be as, if not more, important than genetic factors, as borne out by previous studies [55–57].
325 Purely technical factors in sample collection seem implausible to explain the range of
326 phenotypes we observed. Whilst breeding seasons are unlikely to be the cause (as pigs are
327 nonseasonal), it has been shown that stress and physical trauma can affect spermiogenesis,
328 with stress-induced infertility being previously been reported in mice, boars and humans
329 [56,58,59]. Although chromatin integrity is important for fertility [60], morphological
330 differences head shapes are not directly due to chromatin integrity in stud boar sperm [19]
331 or in humans [61] [62] except in the very round sperm examples seen in very few of in pig
332 samples. This suggests that chromatin integrity is not an important factor in the structure of

333 the main phenotypes, as there are very few other sperm that show known oxidative
334 damage-induced phenotypes. It is unlikely that there would be such a disparity in
335 phenotype representation if they were related.
336
337 *Progressive pig sperm phenotypes match known defects in mechanisms of spermiogenesis*
338 The sperm were organised into three groups that illustrate the progressive abnormalities
339 (Figure 3). These are (1) extrusion of a basal spike; (2) basal compression, developing
340 asymmetrically; and (3) basal compression with failure of the remainder of the nucleus to
341 elongate. Potential mechanisms that can generate these phenotypes have been described in
342 mice, and information from other mammals can be used as an analogue for boar
343 spermatogenesis [63,64].
344
345 The elongation of the nucleus is shaped by five core elements. First, the ectoplasmic
346 specialisation of the Sertoli cell, which provides compressive forces externally [65,66].
347 Second, the acroplaxome (a cytoskeletal plate composed of f-actin and keratin) upon which
348 the Sertoli cell pushes for nuclear elongation [65,67,68]. Third, the Sertoli cell-spermatid
349 linkers (afadin/nectin complexes) which transmit the forces from the Sertoli cell [69].
350 Fourth, the manchette (a network of microtubules around the base of the sperm head)
351 which directs the basal nuclear structure and tail attachment [52,70,71]. Fifth, the groove
352 belt (the connection between the machete and the nucleus where the acroplaxome ends;
353 [52,70,71]. These components are interconnected, and while not the only mediators of
354 sperm shape, they are important for understanding how perturbations to the process of
355 elongation in spermiogenesis can cause sperm defects. Many proteins are involved in

356 spermatid elongation; SUN3, SUN4 and SUN5 are of particular importance in the process of
357 manchette formation and the attachment of the sperm head to the tail. Both SUN3 and
358 SUN4 knockouts result in a phenotype that does not successfully elongate and have a round
359 nucleus with a mispositioned acrosome [70,72,73], with SUN3 knockout also causing
360 complete failure of manchette formation [74]. SUN5 anchors sperm heads to their tails [75]
361 and does not affect the acrosomal attachment [76]. SUN5 knockouts form acephalic
362 spermatozoa [75]; these are unlikely to be the cause of the abnormal sperm in our samples
363 as we did not see these phenotypes. Other proteins are more likely candidates to explain
364 these abnormalities. The dynein and kinesin motor proteins are involved in elongation and
365 the action of the Sertoli cell ectoplasmic specialisation. Dynein knockouts in mice result in
366 continuous deformation of sperm with malformation of the general structure with reduced
367 elongation and poor formation of the structures around the acrosome [77–80]. Kinesins are
368 also involved [65] and knock outs of the kinesin *KIF3A* give rise to bulb-like morphology with
369 over compression of the manchette [52].
370
371 Nectin-2/3 is part of the spermatid-Sertoli cell connections directing the majority of sperm
372 head elongation [65]. Nectin-2/3 disruption in spermatogenesis affects fertility [81], and is
373 linked to environmental changes [56]. Deficiency of Nectin-2 has also been shown to give a
374 diverse range of abnormal sperm in mice similar to the general structural abnormality
375 shown in the pig sperm [82].
376

377 Whilst Figure 3 showed the progression of phenotypes with increasing severity, we outline

378 the structural elements that influence sperm shape in Figure 5 and indicate the forces that

379 may be operating on the developing sperm to generate these phenotypes.

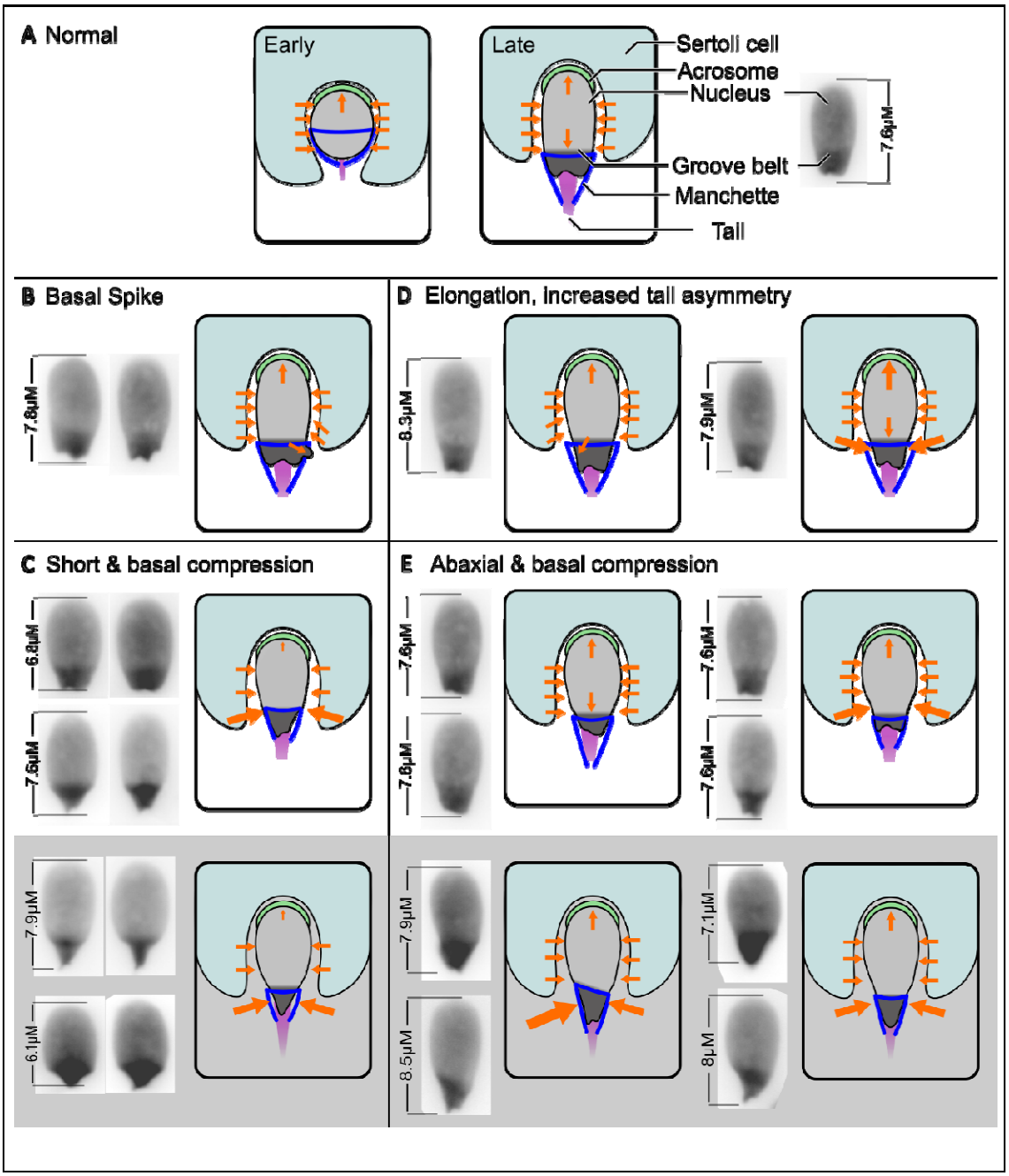

Figure 5 – Summary of the forces involved in shaping the sperm nucleus and the abnormal phenotypes we observe. (A) the normal forces of elongation of a pig sperm exerted on and generated within the cell by the Sertoli cell ectoplasmic specialisation. The Basal spike (B) section shows the forces happening to the cells with an anterior bulge around the tail attachment region that is possibly either from the force of a broken tail or malformation of the manchette/ ectoplasmic specialisation hoops slipping due to lack of acroplaxome attachment proteins below the manchette forcing out the bulge. The short with basal compression (C)phenotype has concentrated pressure around the base and a lack of intranuclear pressure which could come either from a lack of molecular motors or misalignment of ectoplasmic specialisation hoops that results in a lot of basal pressure causing constriction but not the elongation seen in other phenotypes. The elongation with increased tail asymmetry (D) is potentially due to manchette misattachment causing the asymmetry that is not severe enough to cause a full abaxial structure or abaxial misalignment of the hoops from the ectoplasmic specialisation without enough constricting force to cause full abaxial development. The elongation of this sperm phenotype is likely due to increased intranuclear pressure from the compression of the manchette and loops that are potentially due to increased molecular motor activity such as dyneins or kinesins or potentially moderated by the same acroplaxome attachment complex that allows for more force transfer due to more attachment. The Abaxial (E) phenotype with basal compression is likely due to a combination of manchette misalignment exacerbated by the basal compression due to the previously mentioned processes.

380

381 We see over compression of the manchette and a dysfunction of nuclear elongation;
382 potentially the absence or reduction in levels of one of these connector proteins or
383 molecular motors would result in over-compression of the manchette and improper
384 elongation [52,82]. One potential mechanism for this could involve the over-tightening of
385 the hoops of the Sertoli cell ectoplasmic specialisation via uneven pressure exerted on the
386 nucleus, either because the hoops lack constricting forces or because they lose their solid
387 connection to the acroplaxome and prevent its function as a modulator of elongation.

388

389 Although we cannot be certain that these are the mechanisms at play in these boar
390 samples, our analysis indicates that these structural changes are localised to specific regions
391 of the sperm. This suggests that further study of the proteins involved in these regions will
392 be important to understanding variation in boar sperm development. Particularly, if the
393 components are affected by environmental factors, there may be possible interventions to
394 improve sperm quality and ejaculate consistency.

395

396 *Implications for the pig breeding industry*

397 This work, and Barquero *et al.* [83] both show a consistent distribution of morphological
398 phenotypes. Barquero *et al.,* however, only used samples comparable to those in our study
399 categorised by breeders as AIS. Given the previously reported link between sperm head size
400 and motility with simple morphological parameters such as height and width [84], and an
401 association between the number of stillbirths in Piétrain boars and poor sperm motility [83],
402 we see clear support for the well-established idea that boar semen quality is significantly

403 affected by the environment [55,57,85]. Further investigation of this relationship is needed,
404 particularly focussing on candidate proteins that can explain the phenotypes; a deeper
405 understanding of sperm morphology may further explain the relationship between
406 morphology, motility and farrowing outcomes.
407
408 Evidence suggests that pig AI may be suboptimal [86–89], with this potentially due to the
409 methods used to classify sperm at AIS or N-AIS. This interpretation is supported in this
410 study, where a large overlap of morphology and the subtle intermediate phenotypes of
411 abnormal sperm between AIS and N-AIS samples is seen. It would therefore be an important
412 next step to test the fertility of samples classified as such using this new approach.
413
414 **Conclusions**
415 In this study we demonstrate that morphometric analysis of pig sperm using NMA software
416 effectively distinguishes morphologically distinct populations of nuclei. Our analysis reveals
417 differences in sperm nucleus morphology between animals classified as commercially
418 acceptable (AIS) and unacceptable (N-AIS) based on assessment to industry standards. Use
419 of NMA has offered additional insights into pig sperm. Importantly, the distribution of
420 sperm phenotypes between different collection dates and between breeds suggests that
421 environmental factors in sperm collection and transport influence can greatly influence
422 sperm morphology and fertility. Further study is needed to understand how these
423 phenotypes develop, and the functional consequences for boar fertility. These methods may
424 also be of use in the categorisation of the phenotypic distributions within human sperm and

have the potential to provide insights into the various complex and subtle morphological differences that could be linked to environmental factors, fertility, and disease.

Acknowledgments

We would like to thank JSR Genetics Ltd. for supplying the samples that were used in this study.

433 **References**

434 1. Agarwal A, Mulgund A, Hamada A, Chyatte MR. 2015 A unique view on male infertility
435 around the globe. *Reprod. Biol. Endocrinol. RBE* **13**, 37. (doi:10.1186/s12958-015-0032-1)
436 2. Organization WH, Geneva. 2021 WHO laboratory manual for the examination and
437 processing of human semen.
438 3. Sharma R, Agarwal A. 2011 Spermatogenesis: An Overview. In *Sperm Chromatin:*
439 *Biological and Clinical Applications in Male Infertility and Assisted Reproduction* (eds A
440 Zini, A Agarwal), pp. 19–44. New York, NY: Springer. (doi:10.1007/978-1-4419-6857-9_2)
441 4. Liu DY, Clarke GN, Baker HWG. 1991 Relationship Between Sperm Motility Assessed with
442 the Hamilton-Thorn Motility Analyzer and Fertilization Rates *In Vitro*. *J. Androl.* **12**, 231–
443 239. (doi:10.1002/j.1939-4640.1991.tb00258.x)
444 5. Donnelly ET, Lewis SEM, McNally JA, Thompson W. 1998 In vitro fertilization and
445 pregnancy rates: the influence of sperm motility and morphology on IVF outcome. *Fertil.*
446 *Steril.* **70**, 305–314. (doi:10.1016/S0015-0282(98)00146-0)
447 6. Moghadam KK, Nett R, Robins JC, Thomas MA, Awadalla SG, Scheiber MD, Williams DB.
448 2005 The Motility of Epididymal or Testicular Spermatozoa Does Not Directly Affect
449 IVF/ICSI Pregnancy Outcomes. *J. Androl.* **26**, 619–623. (doi:10.2164/jandrol.05018)
450 7. Kihaile P, Hirotsuru K, Kumasako Y, Misumi J, Utsunomiya T. 2003 Fertilization rates of
451 small-head sperm in conventional IVF and ICSI. *Arch Androl* **49**.
452 (doi:10.1080/01485010390219692))
453 8. Guzick DS *et al.* 2001 Sperm Morphology, Motility, and Concentration in Fertile and
454 Infertile Men. *N. Engl. J. Med.* **345**, 1388–1393. (doi:10.1056/NEJMoa003005)

455 9. Coetzee K, Kruge TF, Lombard CJ. 1998 Predictive value of normal sperm morphology: A
456 structured literature review. *Hum. Reprod. Update* **4**, 73–82.
457 10. Danis RB, Samplaski MK. 2019 Sperm Morphology: History, Challenges, and Impact
458 on Natural and Assisted Fertility. *Curr. Urol. Rep.* **20**, 43. (doi:10.1007/s11934-019-0911-
459 7)
460 11. Rodríguez AL, Rijsselaere T, Beek J, Vyt P, Soom A, Maes D. 2013 Boar seminal
461 plasma components and their relation with semen quality. *Syst Biol Reprod Med* **59**.
462 (doi:10.3109/19396368.2012.725120))
463 12. Waberski D, Riesenbeck A, Schulze M, Weitze KF, Johnson L. 2019 Application of
464 preserved boar semen for artificial insemination: Past, present and future challenges.
465 *Theriogenology* **137**, 2–7. (doi:10.1016/j.theriogenology.2019.05.030)
466 13. In press. Artificial Insemination (AI) Standard for pigs | AHDB. See
467 https://ahdb.org.uk/knowledge-library/artificial-insemination-ai-standard-for-pigs
468 (accessed on 3 March 2025).
469 14. Roca J, Parrilla I, Rodriguez-Martinez H, Gil M, Cuello C, Vazquez J, Martinez E. 2011
470 Approaches Towards Efficient Use of Boar Semen in the Pig Industry. *Reprod. Domest.*
471 *Anim.* **46**, 79–83. (doi:10.1111/j.1439-0531.2011.01828.x)
472 15. Tardif S, Laforest J-P, Cormier N, Bailey JL. 1999 The importance of porcine sperm
473 parameters on fertility in vivo. *Theriogenology* **52**, 447–459. (doi:10.1016/S0093-
474 691X(99)00142-9)
475 16. O'Connor RE, Fonseka G, Frodsham R, Archibald AL, Lawrie M, Walling GA, Griffin DK.
476 2017 Isolation of subtelomeric sequences of porcine chromosomes for translocation

477 screening reveals errors in the pig genome assembly. *Anim. Genet.* **48**, 395–403.
478 (doi:10.1111/age.12548)
479 17. Maes D, Lopez Rodriguez A, Rijsselaere T, Vyt P, Van Soom A. 2011 Artificial
480 Insemination in Pigs. In *Artificial Insemination in Farm Animals* (ed M Manafi), InTech.
481 (doi:10.5772/16592)
482 18. Holt WV, Van Look KJW. 2004 Concepts in sperm heterogeneity, sperm selection and
483 sperm competition as biological foundations for laboratory tests of semen quality.
484 *Reproduction* **127**, 527–535. (doi:10.1530/rep.1.00134)
485 19. Saravia F, Núñez-Martínez I, Morán JM, Soler C, Muriel A, Rodríguez-Martínez H,
486 Peña FJ. 2007 Differences in boar sperm head shape and dimensions recorded by
487 computer-assisted sperm morphometry are not related to chromatin integrity.
488 *Theriogenology* **68**, 196–203. (doi:10.1016/j.theriogenology.2007.04.052)
489 20. Menkveld R, Wong WY, Lombard CJ, Wetzels AMM, Thomas CMG, Merkus HMWM,
490 Steegers-Theunissen RPM. 2001 Semen parameters, including WHO and strict criteria
491 morphology, in a fertile and subfertile population: An effort towards standardization of
492 in-vivo thresholds. *Hum. Reprod.* **16**. (doi:10.1093/humrep/16.6.1165))
493 21. Van Der Merwe FH, Kruger TF, Oehninger SC, Lombard CJ. 2005 The Use of Semen
494 Parameters to Identify the Subfertile Male in the General Population. *Gynecol. Obstet.*
495 *Invest.* **59**, 86–91. (doi:10.1159/000082368)
496 22. Van Waart J. 2001 Predictive value of normal sperm morphology in intrauterine
497 insemination (IUI): a structured literature review. *Hum. Reprod. Update* **7**, 495–500.
498 (doi:10.1093/humupd/7.5.495)

499 23. Vicente-Fiel S, Palacín I, Santolaria P, Yániz JL. 2013 A comparative study of sperm
500 morphometric subpopulations in cattle, goat, sheep and pigs using a computer-assisted
501 fluorescence method (CASMA-F). *Anim. Reprod. Sci.* **139**, 182–189.
502 (doi:10.1016/j.anireprosci.2013.04.002)
503 24. Yániz JL, Capistrós S, Vicente-Fiel S, Hidalgo CO, Santolaria P. 2016 A comparative
504 study of the morphometry of sperm head components in cattle, sheep, and pigs with a
505 computer-assisted fluorescence method. *Asian J. Androl.* **18**, 840–843.
506 (doi:10.4103/1008-682X.186877)
507 25. Ostermeier GC, Sargeant GA, Yandell BS, Evenson DP, Parrish JJ. 2001 Relationship of
508 Bull Fertility to Sperm Nuclear Shape. *J. Androl.* **22**, 595–603. (doi:10.1002/j.1939-
509 4640.2001.tb02219.x)
510 26. Genualdo V, Turri F, Pizzi F, Castiglioni B, Marletta D, Iannuzzi A. 2021 Sperm Nuclei
511 Analysis and Nuclear Organization of a Fertile Boar–Pig Hybrid by 2D FISH on Both Total
512 and Motile Sperm Fractions. *Animals* **11**, 738. (doi:10.3390/ani11030738)
513 27. Hirai M, Boersma A, Hoeflich A, Wolf E, Föll J, Aumüller R, Braun J. 2001 Objectively
514 Measured Sperm Motility and Sperm Head Morphometry in Boars (Sus scrofa): Relation
515 to Fertility and Seminal Plasma Growth Factors. *J. Androl.* **22**, 104–110.
516 (doi:10.1002/j.1939-4640.2001.tb02159.x)
517 28. Barquero V, Soler C, Sevilla F, Calderón-Calderón J, Valverde A. 2021 A Bayesian
518 analysis of boar spermatozoa kinematics and head morphometrics and their relationship
519 with litter size fertility variables. *Reprod. Domest. Anim.* **56**, 1024–1033.
520 (doi:10.1111/rda.13946)

521 29. Rathje CC *et al.* 2019 Differential Sperm Motility Mediates the Sex Ratio Drive
522 Shaping Mouse Sex Chromosome Evolution. *Curr. Biol.* **29**, 3692-3698.e4.
523 (doi:10.1016/j.cub.2019.09.031)
524 30. BM S. 2019 A high-throughput method for unbiased quantitation and categorization
525 of nuclear morphology. *Biol Reprod* **100**. (doi:10.1093/biolre/ioz013))
526 31. Martinez G *et al.* 2022 Oligogenic heterozygous inheritance of sperm abnormalities
527 in mouse. *eLife* **11**, e75373. (doi:10.7554/eLife.75373)
528 32. Stark-Dykema ER, Dulka EA, Gerlinger ER, Mueller JL. 2022 X-linked palindromic gene
529 families 4930567H17Rik and Mageb5 are dispensable for male mouse fertility. *Sci. Rep.*
530 **12**, 8554. (doi:10.1038/s41598-022-12433-9)
531 33. Skinner BM. 2022 Nuclear Morphology Analysis 2.0.0: Improved image analysis
532 software for measuring nuclear shape. *J. Open Source Softw.* **7**, 4767.
533 (doi:10.21105/joss.04767)
534 34. Hancock J, Hovell G. 1959 The collection of boar semen. *Vet. Rec.* **71**, 664–665.
535 35. In press. R: The R Project for Statistical Computing. See https://www.r-project.org/
536 (accessed on 28 May 2024).
537 36. McInnes L, Healy J, Melville J. 2020 UMAP: Uniform Manifold Approximation and
538 Projection for Dimension Reduction. (doi:10.48550/arXiv.1802.03426)
539 37. Konopka T. 2023 umap: Uniform Manifold Approximation and Projection.
540 38. Ripley B, Venables B, Bates DM, ca 1998) KH (partial port, ca 1998) AG (partial port,
541 polr) DF (support functions for. 2024 MASS: Support Functions and Datasets for Venables
542 and Ripley's MASS.

543 39. Banaszewska D, Andraszek K. 2021 Assessment of the Morphometry of Heads of
544 Normal Sperm and Sperm with the Dag Defect in the Semen of Duroc Boars. *J. Vet. Res.*
545 **65**, 239–244. (doi:10.2478/jvetres-2021-0019)
546 40. Wickham H. 2016 *ggplot2*. Cham: Springer International Publishing.
547 (doi:10.1007/978-3-319-24277-4)
548 41. Rathje CC *et al.* 2019 A Conserved Requirement for Fbxo7 During Male Germ Cell
549 Cytoplasmic Remodeling. *Front. Physiol.* **10**, 1278. (doi:10.3389/fphys.2019.01278)
550 42. Hancock JL. 1956 The Morphology of Boar Spermatozoa. *J. R. Microsc. Soc.* **76**, 84–
551 97. (doi:10.1111/j.1365-2818.1956.tb00443.x)
552 43. Kondracki S, Bonaszewska D, Mielnicka C. 2005 The effect of age on the
553 morphometric sperm traits of domestic pigs (Sus scrofa domestica). *Cell. Mol. Biol. Lett.*
554 **10**, 3–13.
555 44. Czubaszek M, Andraszek K, Banaszewska D, Walczak-Jędrzejowska R. 2019 The effect
556 of the staining technique on morphological and morphometric parameters of boar
557 sperm. *PloS One* **14**, e0214243. (doi:10.1371/journal.pone.0214243)
558 45. Kawarasaki T, Enya S, Otake M. 2022 Sperm Characteristics in Microminipigs. *Vivo*
559 *Athens Greece* **36**, 731–737. (doi:10.21873/invivo.12759)
560 46. Rousso D, Kourtis A, Mavromatidis G, Gkoutzioulis F, Makedos G, Panidis D. 2002
561 Pyriform Head: A Frequent but Little-Studied Morphological Abnormality of Sperm. *Arch.*
562 *Androl.* **48**, 267–272. (doi:10.1080/01485010290031574)
563 47. Kawarsky SJ, Stubbings RB, Basrur PK, King WA. 1995 Pyriform bovine spermatozoa
564 and fertilization potential. *Can. Vet. J.* **36**, 434–436.

565 48. Thundathil J, Palasz AT, Mapletoft RJ, Barth AD. 1999 An investigation of the
566 fertilizing characteristics of pyriform-shaped bovine spermatozoa. *Anim. Reprod. Sci.* **57**,
567 35–50. (doi:10.1016/S0378-4320(99)00058-5)
568 49. Walters AH, Eyestone WE, Saacke RG, Pearson RE, Gwazdauskas FC. 2004 Sperm
569 Morphology and Preparation Method Affect Bovine Embryonic Development. *J. Androl.*
570 **25**, 554–563. (doi:10.1002/j.1939-4640.2004.tb02826.x)
571 50. Shojaei Saadi HA. 2013 Proteins associated with critical sperm functions and sperm
572 head shape are differentially expressed in morphologically abnormal bovine sperm
573 induced by scrotal insulation'. *J. Proteomics* **82**, 64–80. (doi:10.1016/j.jprot.2013.02.027.)
574 51. Boe-Hansen GB, Fortes MRS, Satake N. 2018 Morphological defects, sperm DNA
575 integrity, and protamination of bovine spermatozoa. *Andrology* **6**, 627–633.
576 (doi:10.1111/andr.12486)
577 52. Lehti MS, Kotaja N, Sironen A. 2013 KIF3A is essential for sperm tail formation and
578 manchette function. *Mol. Cell. Endocrinol.* **377**, 44–55. (doi:10.1016/j.mce.2013.06.030)
579 53. Kondracki S, Banaszewska D, Wysokińska A, Chomicz J. 2006 Sperm morphology of
580 cattle and domestic pigs. *Reprod. Biol.* **6 Suppl 2**, 99–104.
581 54. García-Vázquez FA, HERNÁNDEZ-CARAVACA I, MATÁS C, SORIANO-ÚBEDA C, ABRIL-
582 SÁNCHEZ S, IZQUIERDO-RICO MJ. 2015 Morphological study of boar sperm during their
583 passage through the female genital tract. *J. Reprod. Dev.* **61**, 407–413.
584 (doi:10.1262/jrd.2014-170)
585 55. Corcuera BD, Hernández-Gil R, De Alba Romero C, Martín Rillo S. 2002 Relationship
586 of environment temperature and boar facilities with seminal quality. *Livest. Prod. Sci.* **74**,
587 55–62. (doi:10.1016/S0301-6226(01)00286-X)

588 56. LI T, YAO J, ZHANG Q, LI Q, LI J, WANG X, LI W, CHEN A, YAN J. 2020 Chronic Stress
589 Impairs Male Spermatogenesis Function and Nectin-3 Protein Expression in the Testis.
590 *Physiol. Res.* **69**, 297–306. (doi:10.33549/physiolres.934287)
591 57. Kunavongkrit A, Suriyasomboon A, Lundeheim N, Heard TW, Einarsson S. 2005
592 Management and sperm production of boars under differing environmental conditions.
593 *Theriogenology* **63**, 657–667. (doi:10.1016/j.theriogenology.2004.09.039)
594 58. Collodel G, Moretti E, Fontani V, Rinaldi S, Aravagli L, Saragò G, Capitani S, Anichini C.
595 2008 Effect of emotional stress on sperm quality. *Indian J. Med. Res.* **128**, 254–261.
596 59. Lopez Rodriguez A, Van Soom A, Arsenakis I, Maes D. 2017 Boar management and
597 semen handling factors affect the quality of boar extended semen. *Porc. Health Manag.*
598 **3**, 15. (doi:10.1186/s40813-017-0062-5)
599 60. Banaszewska D, Andraszek K, Biesiada-Drzazga B. 2015 Evaluation of sperm
600 chromatin structure in boar semen. *Bull. Vet. Inst. Pulawy* **59**, 271–277.
601 (doi:10.1515/bvip-2015-0040)
602 61. Aziz N, Saleh RA, Sharma RK, Lewis-Jones I, Esfandiari N, Thomas AJ, Agarwal A. 2004
603 Novel association between sperm reactive oxygen species production, sperm
604 morphological defects, and the sperm deformity index. *Fertil. Steril.* **81**, 349–354.
605 (doi:10.1016/j.fertnstert.2003.06.026)
606 62. Nguyen HTT, Dang HNT, Nguyen TTT, Nguyen TV, Dang TC, Nguyen QHV, Le MT.
607 2022 Correlations between abnormalities of morphological details and DNA
608 fragmentation in human sperm. *Clin. Exp. Reprod. Med.* **49**, 40–48.
609 (doi:10.5653/cerm.2021.04777)

610 63. Frankenhuis MT, Kramer MF, De Rooij DG. 1982 Spermatogenesis in the boar. *Vet. Q.*
611 **4**, 57–61. (doi:10.1080/01652176.1982.9693840)
612 64. França LR, Avelar GF, Almeida FFL. 2005 Spermatogenesis and sperm transit through
613 the epididymis in mammals with emphasis on pigs. *Theriogenology* **63**, 300–318.
614 (doi:10.1016/j.theriogenology.2004.09.014)
615 65. Kierszenbaum AL, Tres LL. 2004 The acrosome-acroplaxome-manchette complex and
616 the shaping of the spermatid head. *Arch. Histol. Cytol.* **67**, 271–284.
617 (doi:10.1679/aohc.67.271)
618 66. Yan HHN. 2007 Ectoplasmic specialization: a friend or a foe of spermatogenesis?'.
619 *BioEssays News Rev. Mol. Cell. Dev. Biol.* **29**, 36–48. (doi:10.1002/bies.20513.)
620 67. Kierszenbaum AL, Tres LL, Rivkin E, Kang-Decker N, van Deursen JMA. 2004 The
621 acroplaxome is the docking site of Golgi-derived myosin Va/Rab27a/b- containing
622 proacrosomal vesicles in wild-type and Hrb mutant mouse spermatids. *Biol. Reprod.* **70**,
623 1400–1410. (doi:10.1095/biolreprod.103.025346)
624 68. Zakrzewski P, Rędowicz MJ, Buss F, Lenartowska M. 2020 Loss of myosin VI
625 expression affects acrosome/acroplaxome complex morphology during mouse
626 spermiogenesis†. *Biol. Reprod.* **103**, 521–533. (doi:10.1093/biolre/ioaa071)
627 69. Kierszenbaum A, Rivkin E, Tres L. 2007 Molecular biology of sperm head shaping.
628 *Soc. Reprod. Fertil. Suppl.* **65**, 33–43.
629 70. Yang K. 2018 Ultra-structure of the sperm head-to-tail linkage complex in the
630 absence of the spermatid-specific LINC component SPAG4'. *Histochem. Cell Biol.* **150**, 49–
631 59. (doi:10.1007/s00418-018-1668-7.)

632 71. Tapia Contreras C, Hoyer-Fender S. 2019 CCDC42 Localizes to Manchette, HTCA and
633 Tail and Interacts With ODF1 and ODF2 in the Formation of the Male Germ Cell
634 Cytoskeleton. *Front. Cell Dev. Biol.* **7**.
635 72. Calvi A, Wong ASW, Wright G, Wong ESM, Loo TH, Stewart CL, Burke B. 2015 SUN4 is
636 essential for nuclear remodeling during mammalian spermiogenesis. *Dev. Biol.* **407**, 321–
637 330. (doi:10.1016/j.ydbio.2015.09.010)
638 73. Pasch E, Link J, Beck C, Scheuerle S, Alsheimer M. 2015 The LINC complex component
639 Sun4 plays a crucial role in sperm head formation and fertility. *Biol. Open* **4**, 1792–1802.
640 (doi:10.1242/bio.015768)
641 74. Gao Q. 2020 The testis-specific LINC component SUN3 is essential for sperm head
642 shaping during mouse spermiogenesis'. *J. Biol. Chem.* **295**, 6289–6298.
643 (doi:10.1074/jbc.RA119.012375.)
644 75. Shang Y *et al.* 2017 Essential role for SUN5 in anchoring sperm head to the tail. *eLife*
645 **6**, e28199. (doi:10.7554/eLife.28199)
646 76. Yassine S, Escoffier J, Nahed RA, Pierre V, Karaouzene T, Ray PF, Arnoult C. 2015
647 Dynamics of Sun5 Localization during Spermatogenesis in Wild Type and Dpy19l2 Knock-
648 Out Mice Indicates That Sun5 Is Not Involved in Acrosome Attachment to the Nuclear
649 Envelope. *PLOS ONE* **10**, e0118698. (doi:10.1371/journal.pone.0118698)
650 77. Guttman JA, Kimel GH, Vogl AW. 2000 Dynein and plus-end microtubule-dependent
651 motors are associated with specialized Sertoli cell junction plaques (ectoplasmic
652 specializations). *J. Cell Sci.* **113**, 2167–2176. (doi:10.1242/jcs.113.12.2167)

653 78. Wen Q. 2018 Dynein 1 supports spermatid transport and spermiation during
654 spermatogenesis in the rat testis'. *Am. J. Physiol.-Endocrinol. Metab.* **315**, 924–948.
655 (doi:10.1152/ajpendo.00114.2018.)
656 79. Yang Z *et al.* 2019 Dynein axonemal intermediate chain 2 plays a role in
657 gametogenesis by activation of Stat3. *J. Cell. Mol. Med.* **23**, 417–425.
658 (doi:10.1111/jcmm.13945)
659 80. Zhou S *et al.* 2023 DRC3 is an assembly adapter of the nexin-dynein regulatory
660 complex functional components during spermatogenesis in humans and mice. *Signal*
661 *Transduct. Target. Ther.* **8**, 1–4. (doi:10.1038/s41392-022-01293-4)
662 81. Inagaki M, Irie K, Ishizaki H, Tanaka-Okamoto M, Miyoshi J, Takai Y. 2006 Role of cell
663 adhesion molecule nectin-3 in spermatid development. *Genes Cells* **11**, 1125–1132.
664 (doi:10.1111/j.1365-2443.2006.01006.x)
665 82. Mueller S, Rosenquist TA, Takai Y, Bronson RA, Wimmer E. 2003 Loss of Nectin-2 at
666 Sertoli-Spermatid Junctions Leads to Male Infertility and Correlates with Severe
667 Spermatozoan Head and Midpiece Malformation, Impaired Binding to the Zona Pellucida,
668 and Oocyte Penetration1. *Biol. Reprod.* **69**, 1330–1340.
669 (doi:10.1095/biolreprod.102.014670)
670 83. Barquero V, Roldan ERS, Soler C, Vargas-Leitón B, Sevilla F, Camacho M, Valverde A.
671 2021 Relationship between Fertility Traits and Kinematics in Clusters of Boar Ejaculates.
672 *Biology* **10**, 595. (doi:10.3390/biology10070595)
673 84. Gu N-H, Zhao W-L, Wang G-S, Sun F. 2019 Comparative analysis of mammalian
674 sperm ultrastructure reveals relationships between sperm morphology, mitochondrial
675 functions and motility. *Reprod. Biol. Endocrinol.* **17**, 66. (doi:10.1186/s12958-019-0510-y)

676 85. Colenbrander B, Kemp B. 1990 Factors influencingsemen quality in pigs. *Biosci. Proc.*
677 (doi:10.1530/biosciprocs.13.008)
678 86. Dyck M, Foxcroft G, Novak S, Ruiz-Sanchez A, Patterson J, Dixon W. 2011 Biological
679 Markers of Boar Fertility. *Reprod. Domest. Anim.* **46**, 55–58. (doi:10.1111/j.1439-
680 0531.2011.01837.x)
681 87. Sutovsky P. 2015 New Approaches to Boar Semen Evaluation, Processing and
682 Improvement. *Reprod. Domest. Anim.* **50**, 11–19. (doi:10.1111/rda.12554)
683 88. Jung M, Rüdiger K, Schulze M. 2015 In Vitro Measures for Assessing Boar Semen
684 Fertility. *Reprod. Domest. Anim.* **50**, 20–24. (doi:10.1111/rda.12533)
685 89. Zuidema D, Kerns K, Sutovsky P. 2021 An Exploration of Current and Perspective
686 Semen Analysis and Sperm Selection for Livestock Artificial Insemination. *Anim. Open*
687 *Access J. MDPI* **11**, 3563. (doi:10.3390/ani11123563)
688